Pharmacological and Functional Comparison of the Polo-like Kinase Family: Insight into Inhibitor and Substrate Specificity

Eric F. Johnson,* Kent D. Stewart, Keith W. Woods, Vincent L. Giranda, and Yan Luo

Cancer Research, Abbott Laboratories, AP9, 100 Abbott Park Road, Abbott Park, Illinois 60064

Received May 8, 2007; Revised Manuscript Received June 20, 2007

ABSTRACT: PLK1 (polo-like kinase 1) is a key mitotic kinase and a therapeutic target in the treatment of proliferative diseases. Here we investigate the relative substrate specificity and pharmacological relatedness of PLK1, -2, -3, and -4 that together comprise a conserved family of Ser/Thr kinases (PLK family). We report consensus substrate sequences for PLK2, -3, and -4 and an expanded consensus sequence for PLK1, which we use to design an optimal peptide substrate, PLKtide. We report inhibitory activity for the entire PLK family across a diverse set of small-molecule ATP-competitive inhibitors including several clinical compounds. With respect to both substrate and ATP-site specificity, highest similarity is observed between PLK2 and PLK3, PLK1 is next most similar, and PLK4 is least similar. Further, we have identified and report time-dependent inhibition by two potent and selective PLK inhibitors.

The polo-like kinase (PLK)[1] family of Ser/Thr kinases is the focus of intensive drug discovery aimed at the treatment of proliferative diseases. The PLK family consists of PLK1, PLK2 (Snk), PLK3 (Fnk, Prk), and PLK4 (Sak), the best characterized of which, PLK1, serves key roles in mitosis and is a well-validated therapeutic target for cancer (*1*−*13*). Less well characterized, the pharmacological implications of PLK2, PLK3, and PLK4 inhibition remain uncertain. Differences in spaciotemporal expression, subcellular localization, substrate specificity, and regulation indicate different functions, although some functional redundancy, in mitosis for example, is observed (*14*−*26*). In the presence of mitotic poisons, PLK2 silencing has been reported to enhance apoptosis and suggested to confer sensitization to Taxol-resistant tumors (*19*). Yet, another report indicates a tumor suppressor function for PLK2 in B cell neoplasia (*16*). Moreover, both PLK2 and PLK3 have been reported to play important nonmitotic roles in neuronal synaptic plasticity (*17*, *18*). PLK3 has been reported to activate p53 in response to oxidative stress and to promote mitotic progression, consistent with its suitability as an antiproliferative target (*21*−*23*). PLK4 has been implicated in the promotion of centriole duplication, cell cycle progression, and induction of apoptosis upon silencing (*20*, *24*). Since PLK2, PLK3, and PLK4 lack the extensive validation associated with PLK1, insight regarding specificity is essential when targeting the PLK family (*1*).

The polo-like kinase family members are characterized by a multidomain structure consisting of a highly conserved N-terminal catalytic domain and a relatively divergent C-terminal polo-box domain (PBD). PLK1−3 contain tandem C-terminal polo-box sequences that are relatively divergent in structure yet have conserved function as phosphopeptide (Ser-pSer/pThr-Pro/X) binding domains that serve to localize these kinases and regulate their activity (*25*, *27*−*29*). PLK4 is most divergent in its C-terminus, containing only a single polo-box domain that may not function as a substrate docking site but rather as a homodimerization domain (*25*). The PBDs of PLKs are an attractive alternative target for small-molecule inhibitor design as drugs targeting these sites could prove PLK-isoform selective (*1*, *26*).

PLK kinase domains contain many of the conserved features of other protein kinases and have even higher sequence similarity to each other, with PLK2 and PLK3 being most similar and PLK1 and PLK4 most dissimilar (*26*, *30*, *31*). Moreover, the canonical Gly-X-Gly-X-X-*Gly* sequence that typifies the ATP-binding site of most protein kinases is Gly-X-Gly-X-Phe-*Ala* in all four PLKs (*15*, *32*, *33*). The efficacy of a kinase inhibitor depends critically on its specificity toward one or more defined kinase targets. Although kinase specificity cannot be sufficiently predicted by primary sequence homology, a set of diverse compounds may be profiled against a set of kinases to determine structure−activity relationship (SAR) similarity (*34*−*36*). Together, these data provide information regarding inhibitor specificity, tractability of target inhibition, and likely toxicity/polypharmacology that is critical to drug discovery (*34*, *35*).

Despite the large interest in targeting PLKs, little is known of their SAR similarity. While this report was in submission, the crystal structure of a T210V mutant of the PLK-1 catalytic domain appeared in press (*37*). Without structures for PLK2−4 and with that of PLK1 only recently available, current understanding of SAR similarity within the family is limited primarily to modeling predictions. The work presented here investigates substrate and inhibitor specificity directly and provides experimental data to test, complement, and enhance our current understanding of PLK family structure and function. Furthermore, through the course of

* To whom correspondence should be addressed. Tel: 847-936-6344. Fax: 847-938-2365. E-mail: eric.f.johnson@abbott.com.

[1] Abbreviations: PLK, polo-like kinase; PLK-KD, PLK kinase domain; fl-PLK, full-length PLK; PBD, polo-box domain; PDB, Protein Data Bank; SAR, structure−activity relationship; PI3K, phosphoinositol 3-kinase.

10.1021/bi7008745 CCC: $37.00
Published on Web 07/27/2007

these studies we have identified time-dependent inhibition of PLK1 by the relatively selective and potent PLK1 inhibitors wortmannin and BI-2536, providing important insight into their mechanism of action.

EXPERIMENTAL PROCEDURES

Inhibitors. Compounds **4**, **9**, **14**, and **15** (American Custom Chemicals), **6** (Biomol), **7** and **16** (Calbiochem), and **17**−**19** (Sigma) were commercially obtained. The remaining compounds were synthesized according to literature procedures: **1**−**3** (*38*), **5** (*39*, *40*), **8** (*41*, *42*), **10** (*43*, *44*), **11**−**13** (*45*), **20** (*46*, *47*), and **21** (*48*, *49*).

Enzymes and Substrates. GST-tagged PLK1[1−331] (PLK1-KD) was expressed in SF9 cells using a baculoviral expression system and affinity purified using glutathione−Sepharose and S-Sepharose Fast Flow resins. His-tagged PLK4[1−269] (PLK4-KD) was expressed in *Escherichia coli* and purified using nickel-resin. Baculovirus-expressed GST-His-tagged Snk (fl-PLK2) (Cell Signaling Technology) and His-tagged PLK3[19−301] (PLK3-KD) (Upstate) were commercially obtained. The peptide library employed was the Jerini general kinase substrate set, comprising 720 biotinylated peptides derived from human phosphorylation sites containing 1331 serine, 650 threonine, and 370 tyrosine residues (JPT Peptide Technologies, GmbH). All other peptides were custom synthesized (Genemed) and were of the form biotin−C_6 linker−peptide−CO_2H.

PLK Kinase Assays and K_i Determination. Unless otherwise specified, kinase assays were conducted as follows with final concentrations as indicated. In 384-well polypropylene plates (Axygen), 10 μL of compound (2% DMSO) was mixed with 10 μL of kinase and biotinylated peptide substrate (2 μM), followed by immediate initiation with 10 μL of [λ-^{33}P]ATP (5 μM, 2 mCi/μmol) (Perkin-Elmer) using a reaction buffer comprising 25 mM HEPES, pH 7.5, 0.5 mM DTT, 10 mM $MgCl_2$, 100 μM Na_3VO_4, and 0.075 mg/mL Triton X-100. Reactions were quenched after 1 h by the addition of 50 μL of stop buffer (50 mM EDTA, 2 M NaCl). Eighty microliters of the stopped reactions was transferred to 384-well streptavidin-coated plates (FlashPlate Plus; Perkin-Elmer), incubated for 30 min at room temperature, washed three times with 0.05% Tween-20/PBS using an ELX-405 automated plate washer (BioTek), and counted on a TopCount scintillation plate reader (Packard). PLK1-KD (2 nM), fl-PLK1 (5 nM), fl-PLK2 (5 nM), and PLK3-KD (0.2 nM) used PLKtide as a substrate. PLK4-KD (2 nM) used peptide A-A11 (TPSDSLIYDDGLS) as a substrate (Jerini AG). Apparent K_m values (5 μM ATP) were 0.2 μM (PLK1-KD), 2 μM (fl-PLK2), 0.8 μM (PLK3-KD), and 10 μM (PLK4-KD) for the corresponding peptide substrates. IC_{50} values were determined using an 11-point, 3-fold dilution series. To normalize affinity data, IC_{50} values were converted to apparent K_i assuming a Cheng−Prusoff relationship (*50*). In all cases, the estimated K_i and IC_{50} are similar (within 2.5-fold), as ATP concentrations were low relative to apparent ATP K_m values of 100 μM (PLK1-KD), 120 μM (fl-PLK2), 20 μM (PLK3-KD), and 4 μM (PLK4-KD).

Substrate Library Screening and Consensus Analysis. A mixture of PLK1-KD (20 nM), fl-PLK2 (50 nM), PLK3-KD (2.5 nM), or PLK4-KD (20 nM) and [λ-^{33}P]ATP (5 μM, 4 mCi/μmol) was added to two 384-well plates containing 720 biotinylated peptides (50 pmol/well) with a final reaction volume of 25 μL, incubated for 2 h, quenched with 80 μL of stop buffer, and processed per standard PLK protocol (above). Substrates were then rank-ordered by activity (cpm) and those significantly above background (>200 cpm vs 54 ± 34 cpm "no peptide background") used for consensus analysis. Using these criteria, the analysis was conducted with 18, 8, 20, and 19 substrates for PLK1−4, respectively. An initial substrate screen with PLK2 produced questionable results as several robust hits with sequence highly divergent from the observed PLK1 and PLK3 consensus were observed. The kinase activity with these substrates was potently inhibited by staurosporine but not by several specific PLK1/3 inhibitors. We suspected the presence of a trace, but robust, contaminating kinase in this commercial PLK2 prep and repeated the experiment in the presence of 100 nM staurosporine, which suppressed phosphorylation of all substrates except a subset similar or identical to those observed for PLK1/3. The reported consensus is that determined in the presence of 100 nM staurosporine.

Evaluation of Substrates. PLK1-KD (5 nM), fl-PLK2 (10 nM), PLK3-KD (0.1 nM), and [λ-^{33}P]ATP (5 μM, 4 mCi/μmol) were initiated with peptide substrate (2 μM) and stopped at 0, 5, 10, 15, 20, 30, 45, and 60 min. Initial rates were determined from the resulting linear progress curves using Kaleidagraph (Synergy Software), and activity was expressed as percent activity using PLKtide.

Analysis of Time-Dependent Inhibition. Time-dependent inhibition data (progress curves) for inhibition of PLKs by wortmannin and BI 2536 were fit to eq 1 using Kaleidagraph (*51*, *52*):

$$P = P_{max}[1 - e^{-kt}] \quad (1)$$

where P is the amount of product at time (t), P_{max} is the amount of product formed at infinite time, and k is the observed pseudo-first-order binding rate for a given inhibitor concentration. The apparent K_d (K_i') for the reversible binding of wortmannin to PLK1 at 10 μM ATP (<K_m^{ATP}) and the first-order rate of "irreversible" incorporation once bound, k_{inact}, were determined by fitting the resulting pseudo-first-order observed binding rates, k_{obs}, vs corresponding wortmannin concentration, [I], using eq 2 (*51*, *52*):

$$k_{obs} = k_{inact}[I]/(K_i' + [I]) \quad (2)$$

For BI 2536, pseudo-first-order observed binding rates, k_{obs}, obtained at 10 μM ATP (<K_m) and corresponding inhibitor concentrations, [I], were fit to eq 3 in order to estimate the on rate, k_{on} (*53*):

$$k_{obs} = k_{on}[I] + k_{off} \quad (3)$$

Estimation of BI 2536 Off Rate from IC_{50} and k_{on}. Theoretical maximum k_{off} values for BI 2536 from PLK1 were estimated using eq 4, $K_i^{app} = 0.13$ nM (from minimum observed IC_{50} after 4 h preincubation, where BI 2536 may be titrating active sites), and $k_{on} = 0.0049$ min^{-1} nM^{-1} as determined at 10 μM ATP (<K_m) (*53*):

$$K_i = k_{off}/k_{on} \quad (4)$$

Hierarchical Clustering and Multidimensional Analysis. Hierarchical relationships for both substrate and inhibitor specificity were determined by the "complete linkage" clustering method using a "correlation" similarity measure in Spotfire DecisionSite 8.0 (Spotfire, Inc.). For substrate specificity, pairwise similarity was calculated by counting the number of peptides that were common substrates or nonsubstrates for each kinase pair divided by the total number of peptides tested. For inhibitor specificity, pairwise similarity was calculated as the pharmacological interaction strength for each kinase pair as described in Hopkins et al. using a potency threshold of 1.0 log unit (*54*). Multidimensional scaling (MDS) analyses were performed within Microsoft Excel using the XLSTAT plug-in.

Modeling. Sequence alignments were carried out with the BESTFIT utility (Wisconsin Package; Accelrys Inc., San Diego, CA). Homology models of PLK1−4 were constructed using the HOMOLOGY software package (Accelrys). PDB entry 1ATP (protein kinase A) was selected as a template because of its accurate representation of the general structural features of known ATP- and substrate-binding sites. DELPHI calculations (neutral pH) were carried out within the INSIGHT software (Accelrys). Models of PLKtide, wortmannin, and staurosporine bound to PLK1 were created using the corresponding binding modes observed in PDB entries 1PKA, 1E7U, and 1STC for PKI/PKA, wortmannin/PI3K, and staurosporine/PKA, respectively, as templates.

RESULTS

Peptide Library Screening and Substrate Optimization. To identify PLK substrates, we screened each polo-like kinase in vitro against a library of 720 peptides derived from human phosphorylation sites containing 1331 serine, 650 threonine, and 370 tyrosine residues (JPT Peptide Technologies GmbH). PLK1 phosphorylated 18 peptides with significant activity. We aligned these with several substrates described in the literature and an in vitro PLK1 substrate, cJun peptide, previously identified in our laboratories (Figure 1A) (*55*−*59*). Since many of the substrates in the peptide library contain multiple serine or threonine residues, an assumption on the site of phosphorylation by PLK1 was made considering a crude consensus sequence, D/E-X-S/T-ψ-X-D/E (ψ is any hydrophobic amino acid) (*59*). From the resulting alignment, the amino acid frequency at each position was determined and used to generate an expanded PLK1 consensus sequence (Figure 1B). Several peptides were designed having 16 amino acids before and 6 amino acids after the PLK1 phosphorylation site. These peptides comprise the consensus amino acid at the −7 to +7 positions and contain the corresponding Myt1 or Cdc25C (Ser 198) parent amino acids at remaining positions. An improved substrate for PLK1, here termed PLKtide, was identified which corresponds to the consensus sequence for positions −7 to +6 supplemented with residues from Cdc25C for positions −23 to −8.

We identified the predominant consensus sequence from the set of substrates identified for each PLK2−4 and compared them to that of PLK1 (Figure 2A). The observed PLK2 and PLK3 consensus sequences are very similar and contain acidic residues at most of the flanking positions while that for PLK4 indicates a preference for other amino acid residues. Specifically, the PLK4 consensus included a basic residue at −3 (37%), an acidic residue at −2 (50%), Tyr or hydrophobic (ψ) at +1 (47%) and +2 (89%), and Ser/Thr (42%) or Ala (26%) at +4. To further assess relatedness in substrate specificity, we performed hierarchical clustering and multidimensional scaling analysis using the data obtained on the 45 library peptides found to be a substrate for at least one PLK. The results indicate highest similarity in the substrate specificity of PLK2 and PLK3, which differ slightly from that of PLK1, all of which are quite different from that of PLK4 (Figure 2A and B).

The phosphorylation site preference was further investigated in Cdc25C peptide, cJun peptide, and PLKtide. Since PLKtide and the Cdc25C peptide from which it was derived contain multiple potential phosphorylation sites, we also included C-terminal and N-terminal fragments of each along with corresponding site-directed substitutions at putative phosphorylation sites (Figure 2D). Whereas PLK1 and PLK3 preferentially phosphorylated Ser 198 and 191, respectively, in the parent peptide Cdc25C(182−204), all PLKs displayed greatly enhanced activity and a strong preference for the residue corresponding to Ser198 in the optimized substrate (Figure 2E). Further, a strong preference of PLK1 versus PLK2/3 is observed in the utilization of the cJun peptide. PLK4 was not observed to phosphorylate any of these substrates.

Protein 3D Modeling. The sequence alignment of the catalytic domains of PLK1−4 is provided in Chart 1. The pairwise identities of the catalytic domains are shown in Table 1. Homology models of each enzyme permitted the identification of 29 ATP-site binding residues used in calculating the pairwise identities of the ATP-binding sites (listed in Table 1). The highest identities were observed between PLK2 and PLK3, and the lowest identities were observed between PLK1 and PLK4. Pronounced differences in the surface electrostatic properties of the four enzymes were observed, and the DELPHI surfaces are shown in Figure 3A−D. While a significant electropositive region surrounds the ATP- and substrate-binding regions of PLK1−3, a significantly diminished electropositive region exists for PLK4.

Substrate Specificity Modeling. On the basis of homology modeling, Lowery et al. previously predicted similar substrate specificity for PLK1−3 that they expected might differ significantly from that of PLK4 (*25*). Our data provide experimental evidence in agreement with their predictions yet also indicate additional subtleties in substrate specificity within PLK1−3 and which expand consensus sequence contribution beyond the reported D/E-X-S/T-ψ-X-D/E motif (*59*). To extend this analysis, models of PLKtide bound to the substrate region of PLK1−4 were created; the model with PLK1 is shown in Figure 3E. The pronounced preference for negatively charged residues in the PLK substrates is nicely rationalized by the significant electropositive environment of the PLK substrate-binding sites (Figure 3E). The following comments are limited to the protein regions surrounding the substrate P_1, P_2, and P_{-3} side chains, as these are sites that give pronounced differences in substrate sequence preference within the PLK family. The side chain of P_1 projects into a hydrophobic pocket comprised of Leu 211, Leu 256, and Tyr 260. This pocket is similar in PLK2−3 but is significantly deepened in PLK4 with the replacement

A

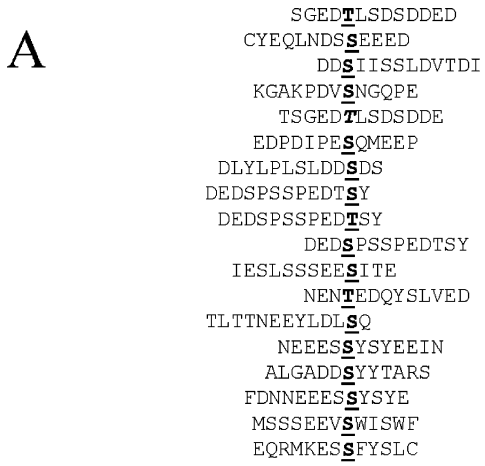

AKMETTFYDDALNASFLPSEGPYGYSNPK	C-jun
AKMETTFYDDALNASFLPSE	c-jun
SPEPILVDTASPSPMETSGCAPAEEDLCQAFSDVILAVNDVDAED	CYCLIN B
LVDTASPSPMETSGCAPAEEDLCQAFSDVILAVNDVDAED	CYCLIN B
GNIDDSLIGGNASAEGPEGE	TCTP
NASAEGPEGEGTESTVITGVDIV	TCTP
NLGEDQAEEISDELMEFSLKDQELKDQEAKVSRSGLYRSPSMPEN	Cdc25C
NLGEDQAEEISDELMEFSLKDQEAKVSRSGLYRSPSMPEN	Cdc25C
GSFPSFEPRNLLSLFEDTLDPT	Myt1 495
PPATPPGSPPCSLLLDSSLSSNWDDDSLGPSL	Myt1 426
PKHISESLGAEVDPDMSWSSSLATPPTLSSTVLIVR	BRCA2 S193
PKHISESLGAEVDPDMSWSSSLATPPTLSSTVLIVRNEEA	BRCA2 T203
HISESLGAEVDPDMSWSSSLATPPTLSSTVLIVRNEEA	BRCA2 S205
ISESLGAEVDPDMSWSSSLATPPTLSSTVLIVRNEEA	BRCA2 S206
SESLGAEVDPDMSWSSSLATPPTLSSTVLIVRNEEA	BRCA2 T207

B

Frequencies at −7 to +7 positions (%):

-7: Total 23, S: 21.7, E: 13, P: 13.
-6: Total 24, D: 20.8, P: 16.7, S: 16.7.
-5: Total 28, S: 21.4, L: 17.8, P: 10.7.
-4: Total 29, S: 20.7, L: 13.8, P: 13.8, E: 10.7, A: 10.7.
-3: Total 31, E: 16.1, L: 16.1, P: 12.9, M: 9.7.
-2: Total 32, E: 46.9, D: 28.1.
-1: Total 32, D: 28.1, S: 21.9, E: 9.4.
+1: Total 32, L: 21.9, Y: 12.5, F: 9.4.
+2: Total 30, S: 26.7, Y: 13.3, I: 10.
+3: Total 28, S: 21.4, E: 14.3, D: 14.3, P: 10.7, L: 10.7.
+4: Total 28, E: 21.4, D: 7.1, L: 7.1, R: 7.1, V: 7.1.
+5: Total 26, D: 19.2, L: 15.4, V: 15.4.
+6: Total 22, E: 18.2, N: 18.2, V: 9.1, T: 9.1, S: 9.1, D: 9.1.
+7: Total 20, E: 20.0, N: 20.0, D: 10.0.

Consensus S-D-X-X-ψ/E-E/D-E/D/S-**S/T**-ψ-S/ψ-S/E/D-E-D/ψ-E/N-E.

Plktide: LGEDQAEEISDDLLED**S**LSDEDE

FIGURE 1: Expanded PLK1 consensus. (A) The top 18 PLK1 substrates identified from peptide library screening and established PLK1 phosphorylation sites of known substrates were used for consensus analysis. (B) The amino acid frequency at each position was used to generate an expanded PLK1 consensus sequence and identify an optimal PLK1 substrate, PLKtide. Putative phosphorylation sites are underlined. Hydrophobic residues are denoted ψ.

of Tyr 260 with Leu. The side chain of P_2 projects into a mixed polarity pocket comprised of Phe 44, Pro 92, and Gln 94 in PLK1−3. This pocket is made more hydrophobic with the replacement of Gln 94 with Met in PLK4. The side chain of P_{-3} projects into a polar region of high variation within the PLK family. In PLK1, the pocket is comprised of Ser 137, Leu 139, Glu 140, and Gly 180. In PLK2/3, these four residues are Ser, Ala, His, and Gly, and in PLK4 these four residues are Glu, Asn, Arg, and Ser. The complexity of polar interactions prevents an unambiguous prediction of substrate preference for the P_{-3} position that would be complementary to this region, but significant variation would be anticipated.

SAR Similarity of PLKs Using ATP Site-Directed Inhibitors. In order to assess and compare inhibitor SAR, we assembled a set of diverse ATP site-directed inhibitors affecting one or more PLKs. Tool compounds were selected through a combination of in-house screening (including various Abbott, commercial, and clinical compounds) and

A

Position:	-4	-3	-2	-1	0	+1	+2	+3	+4
Plk1:	X	ψ / E	E / D	E /D / S	S / T	ψ	S / ψ	S /E / D	E
Plk2:	E	E / D	X	E / D	S / T	E / D	E / D	E / D	E / D
Plk3:	E	E / D	E / D	E / D	S / T	E	E / D	E / D	E / D
Plk4:	X	R / K	E / D	X	S / T	ψ / Y	ψ / Y	X	S / T / A

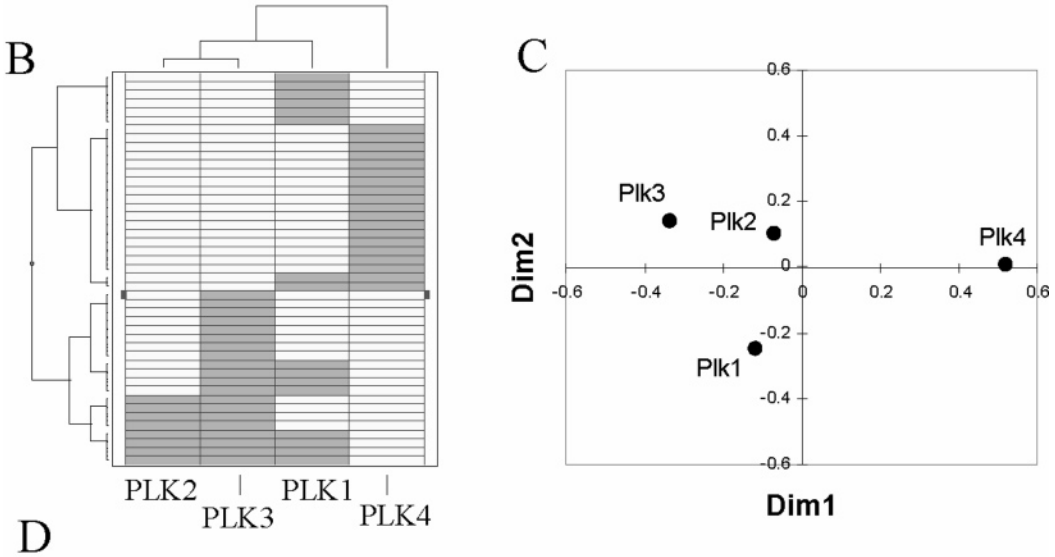

D

S#	Description	Sequence
1	Cdc25C(182-204)	L G E D Q A E E I **S** D E L M E F **S** L K D Q E A
2	Cdc25C(182-197)	L G E D Q A E E I **S** D E L M E F
3	Cdc25C(192-204)	D E L M E F **S** L K D Q E A
4	Plktide(pS191)	L G E D Q A E E I pS D D L L E D **S** L S D E D E
5	Plktide(192-204)	D D L L E D **S** L S D E D E
6	Plktide(182-197)	L G E D Q A E E I **S** D D L L E D
7	Plktide(S191A)	L G E D Q A E E I **A** D D L L E D **S** L S D E D E
8	Plktide(S198A)	L G E D Q A E E I **S** D D L L E D **A** L S D E D E
9	cJun Peptide	A K M E T **T** F Y D D A L N A S F L P S E K K K
10	Plktide	L G E D Q A E E I **S** D D L L E D **S** L S D E D E

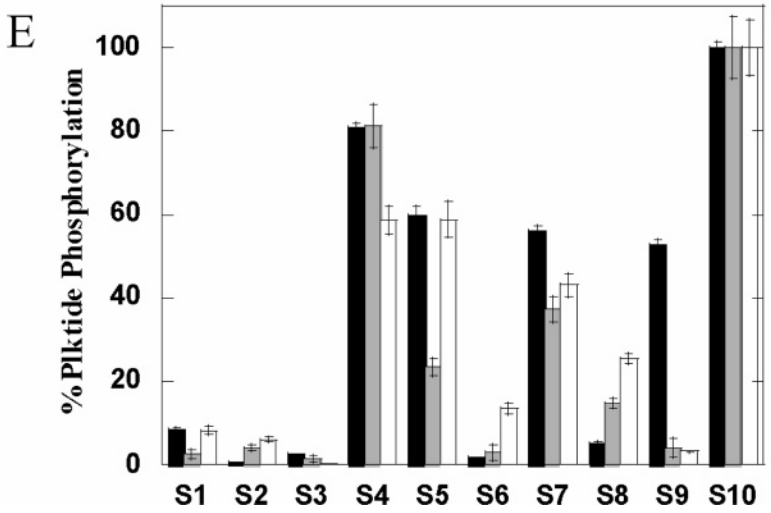

FIGURE 2: Substrate specificity of PLK1−4. (A) Consensus substrate sequences for the Plk family (hydrophobic amino acid denoted ψ). (B) Hierarchical cluster representation of PLK similarity with respect to substrate utilization. All substrates identified from library screening are represented and shaded as active (gray) or inactive (white). (C) Multidimensional scaling analysis showing pairwise distances of the various PLK isoforms as derived from the substrate specificity data in (B). Dim1 and Dim2 are unitless dimensions where distance is inversely proportional to similarity. (D) Substrate sequences, coded S1−10 for simplification, are shown (amino acid numbers correspond to the position in the parent substrate). (E) Relative kinase activity for each substrate as determined by initial rate studies and expressed as percent PLKtide phosphorylation by PLK1 (black bars), PLK2 (gray bars), and PLK3 (white bars).

through a review of the PLK patent and scientific literature. Table 2 summarizes the activity of the compounds against the various family members as determined by in vitro kinase assay. Chemical structures of the compounds are shown in Chart 2. These data were subject to hierarchical clustering analysis providing a "heat map" that depicts SAR relatedness

Chart 1: Sequence Alignment of Catalytic Domains of PLK1−4[a]

```
      51      **  **** *             *  *               100

Plk1  RRYVRGRFLG KGGFAKCFEI SDADTKEVFA GKIVPKSLLL KPHQREKMSM
Plk2  KRYCRGKVLG KGGFAKCYEM TDLTNNKVYA AKIIPHSRVA KPHQREKIDK
Plk3  RTYLKGRLLG KGGFARCYEA TDTETGSAYA VKVIPQSRVV KPHQREKILN
Plk4  EDFKVGNLLG KGSFAGVYRA ESIHSGLEVA IKMIDKKAMY KAGMVQRVQN

      *   *         *              * * * *****  *        149
Plk1  EISIHRSLAH QHVVGFHGFF EDNDFVFVVL ELCRRRSLLE LHKRR.KALT
Plk2  EIELHRILHH KHVVQFYHYF EDKENIYILL EYCSRRSMAH ILKAR.KVLT
Plk3  EIELHRDLQH RHIVRFSHHF EDADNIYIFL ELCSRKSLAH IWKAR.HTLL
Plk4  EVKIHCQLKH PSILELYNYF EDSNYVYLVL EMCHNGEMNR YLKNRVKPFS

      150                        *    ** *         ****199
Plk1  EPEARYYLRQ IVLGCQYLHR NRVIHRDLKL GNLFLNEDLE VKIGDFGLAT
Plk2  EPEVRYYLRQ IVSGLKYLHE QEILHRDLKL GNFFINEAME LKVGDFGLAA
Plk3  EPEVRYYLRQ ILSGLKYLHQ RGILHRDLKL GNFFITENME LKVGDFGLAA
Plk4  ENEARHFMHQ IITGMLYLHS HGILHRDLTL SNLLLTRNMN IKIADFGLAT

      200                                             249
Plk1  KVEYDGERKK TLCGTPNYIA PEVLSKKGHS FEVDVWSIGC IMYTLLVGKP
Plk2  RLEPLEHRRR TICGTPNYLS PEVLNKQGHG CESDIWALGC VMYTMLLGRP
Plk3  RLEPPEQRKK TICGTPNYVA PEVLLRQGHG PEADVWSLGC VMYTLLCGSP
Plk4  QLKMPHEKHY TLCGTPNYIS PEIATRSAHG LESDVWSLGC MFYTLLIGRP

      250                                             299
Plk1  PFETSCLKET YLRIKKNEYS IPKHINPVAA SLIQKMLQTD PTARPTINEL
Plk2  PFETTNLKET YRCIREARYT MPSSLLAPAK HLIASMLSKN PEDRPSLDDI
Plk3  PFETADLKET YRCIKQVHYT LPASLSLPAR QLLAAILRAS PRDRPSIDQI
Plk4  PFDTDTVKNT LNKVVLADYE MPTFLSIEAK DLIHQLLRRN PADRLSLSSV

      300    309
Plk1  LNDEFFTSGY
Plk2  IRHDFFLQGF
Plk3  LRHDFFTKGY
Plk4  LDHPFMSRNS
```

[a] ATP-binding site residues are denoted with an asterisk. Numbering refers to PLK1. Human PLK1−4 sequences refer to residues 51−309, 80−338, 60−318, and 10−269 of SWISSPROT entries PLK1_HUMAN, SNK_HUMAN, CNK_HUMAN, and REFSEQ entry NM_014264, respectively.

Table 1: Pairwise Identity of PLK Catalytic Domains and ATP-Binding Sites[a]

	PLK1	PLK2	PLK3
PLK2	53 (90)		
PLK3	54 (86)	68 (97)	
PLK4	37 (60)	41 (60)	42 (60)

[a] The first number in each box refers to the percent identity within the sequences of the entire catalytic domains. The second number, in parentheses, refers to the percent identity within the ATP-binding site.

with respect to this compound set (Figure 4A). Using multidimensional scaling (MDS) analysis, these data were used to calculate pairwise pharmacological similarity of each PLK in the family (Figure 4B). These data indicate highest SAR similarity between PLK2/3, with PLK1 being next most similar, and PLK4 being least similar.

Inhibition of PLK1−3 by Wortmannin and BI 2536. Our studies using wortmannin indicated that this inhibitor imparts time-dependent inhibition of PLK1. To characterize this, we monitored PLK1 activity at varying wortmannin and ATP concentrations over time. Figure 5A shows progress curves for PLK1 activity in the presence of varying concentrations of wortmannin. Figure 5B is a replot of the observed pseudo-first-order binding rate, k_{obs}, versus wortmannin concentration. These data indicate that wortmannin binds to PLK1 reversibly with an apparent K_d of 2.3 ± 0.5 μM and, when bound, incorporates at a rate of 0.090 ± 0.008 min^{-1}. Although both PLK2 and PLK3 were inhibited by wortmannin with K_i' values comparable to that determined for PLK1, time-dependent inhibition was not observed (data not shown), indicating that PLK1 is the only family member to be covalently modified, within the time scale of these experiments, by wortmannin (Table 2). To investigate inhibition of full-length PLK (fl-PLK1) as well as binding mode, we again monitored the time dependence of inhibition using a fixed wortmannin concentration (2.5 μM) and varying ATP concentrations (5−625 μM) (Figure 5C). As with the PLK1 kinase domain (PLK1-KD), time-dependent inhibition of fl-PLK1 was also observed; further, the pseudo-first-order rate of inhibition decreased as ATP was increased, consistent with an ATP competitive binding mode (k_{obs} = 0.11 ± 0.01 at 5 μM ATP, k_{obs} = 0.078 ± 0.010 at 125 μM ATP, and k_{obs} = 0.051 ± 0.006 at 625 μM ATP). We conducted experiments similar to those described above for wortmannin with BI 2536. Time-dependent inhibition was observed for PLK1, -2, and -3. For PLK1, our experiments indicate an on rate of ~0.0049 ± 0.0006 min^{-1} nM^{-1} ($T_{1/2}$ ~2 h at 1 nM), a *maximum* off rate of 0.00064 min^{-1} ($T_{1/2}$ ≥ 18 h), and a corresponding *minimum* K_i of 130 pM (data not shown).

Modeling the Binding Mode of Wortmannin. A model of the binding mode of wortmannin in PLK1 is shown in Figure 6A. This model is based on the known covalent binding mode of wortmannin interaction with phosphoinositol 3-kinase (PI3K) (*60*). According to this model, Lys 82 of PLK1 covalently modifies wortmannin in analogy with

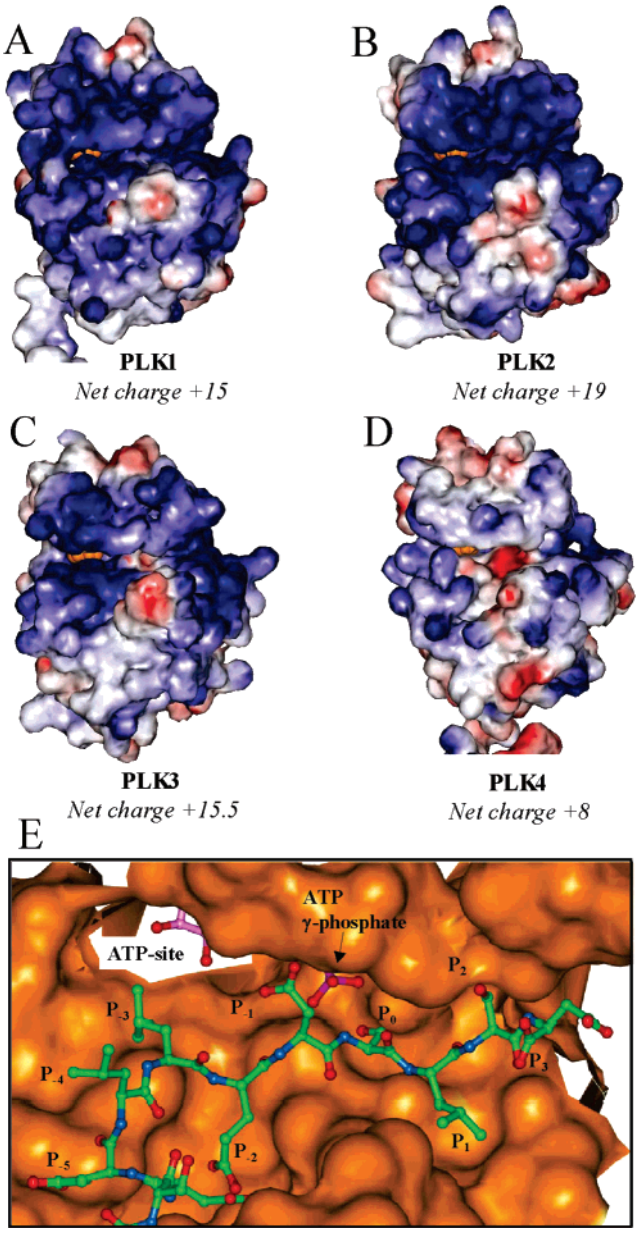

FIGURE 3: Models of PLK1−4. (A−D) DELPHI electrostatic surface diagrams of the charge distribution over the surface of the catalytic domains of PLK1 (A), PLK2 (B), PLK3 (C), and PLK4 (D). Blue surface represents a positively charged region, red surface represents a negatively charged region, and white represents a neutral region. The proteins are derived from homology models based on protein kinase A. The view shows the N-terminal domain oriented to the top and C-terminal domain to the bottom. A model of ATP is included as a small orange surface near the middle of the four images. PLK1−3 are similar in having a significant positively charged region distributed over a large degree of surface area of the proteins. PLK4 diverges from PLK1−3 with a more mixed distribution of charges and a less positive net charge. (E) Model of PLKtide bound to PLK1. Residues P_{-5} to P_{+3} of PLKtide (green atoms) are shown in a bound complex with PLK1 (orange surface). A model of ATP is shown in pink at the top of the image. The λ-phosphate of ATP is visible and is proximal to the P_0 Ser of PLKtide.

the adduct between Lys 833 of PI3K and wortmannin. Binding includes (1) a reversible hydrogen bond interaction between the keto carbonyl and the hinge residue Cys 133 of PLK1, (2) van der Waals contact between the two methyl groups of wortmannin with Cys 67 (Figure 6B), and (3) an irreversible enamine adduct with Lys 82. If this proposed binding mode applies to the other PLK family members, then the observed enzyme specificity can be rationalized. Cys 67 of PLK1 is retained as Cys in PLK2 and PLK3 where weak reversible binding similar to PLK1 is observed. Cys 67 of PLK1 is replaced with a larger Val in PLK4, and steric clash prevents reversible binding in this enzyme (Figure 6C). The basis for the lack of time-dependent inhibition by wortmannin toward PLK2 and PLK3 under our experimental conditions is unclear. We speculate that the time-dependent inhibition of PLK1−3 exhibited by BI 2536, compound **23**, also involves contributions from Cys 133, Cys 67, and Lys 82, but their exact role is currently unknown.

Table 2: K_i Values (μM) for Various Inhibitors against PLK1−4

compd	PLK1	PLK2	PLK3	PLK4
1	>20	>20	>20	9.2
2	>20	>20	>20	0.54
3	>20	0.064	0.21	0.13
4	>20	30	>20	0.24
5	>20	>20	>20	0.12
6	>20	>20	>20	0.79
7	>20	>20	>20	0.12
8	>20	>20	>20	0.0042
9	>20	9.3	>20	0.30
10	>20	0.85	>20	1.4
11	>20	>20	>20	8.9
12	10	0.98	2.7	0.44
13	31	0.14	0.95	0.97
14	>20	18	>20	2.2
15	>20	>20	>20	0.011
16	>8	>19	>16	0.0034
17	0.79	0.15	1.2	0.0026
18	6.1	16	7.5	>20
19	1.5[b]	2.8	3.0	>20
20	0.0048	0.0038	0.0080	0.163
21	<0.001[a]	<0.001[a]	<0.001[a]	>20

[a] Time-dependent inhibition. [b] Time-dependent irreversible inhibition.

ATP Site-Directed Inhibitors. Staurosporine, compound **17**, inhibits all of the PLK enzymes. The inhibitory potencies are near 1 μM for PLK1−3 and low nanomolar for PLK4. Inspection of a model of staurosporine bound to PLK4 (Figure 6D) provides a rationale for this family specificity. Glu 95 of PLK4 (corresponds to residue 137 of PLK1) is optimally positioned to provide a favorable polar interaction with the secondary amine of staurosporine. PLK1−3 have Ser at this corresponding position and would not be expected to present such a favorable binding environment. This selectivity for PLK4 is further accentuated in the staurosporine analogue, GO6976, compound **16**, which retains PLK4 activity but loses PLK1−3 activity by at least an order of magnitude, relative to staurosporine.

This profile of selective inhibition of PLK4 relative to PLK1−3 observed for compounds **16** and **17** is shared by other benchmark inhibitors **4**, **5**, **7**, **8**, **9**, **14**, **15**, and **18** (see Table 2). The wide chemical diversity present in these nine inhibitors suggests that there is not one single factor that explains the PLK4 preference, but likely multiple factors.

Some SAR trends within congeneric series provide some further insight into how inhibitors interact with the ATP-binding site of the PLK family. PP1, compound **6**, is the prototypical [6.5] heterocyclic kinase inhibitor, inspired by the purine ring system of ATP. The PLK4-selective profile of this compound is similar to the compounds reported above, although the PLK4 potency of 0.8 μM is relatively weak. A

Chart 2: PLK Inhibitors

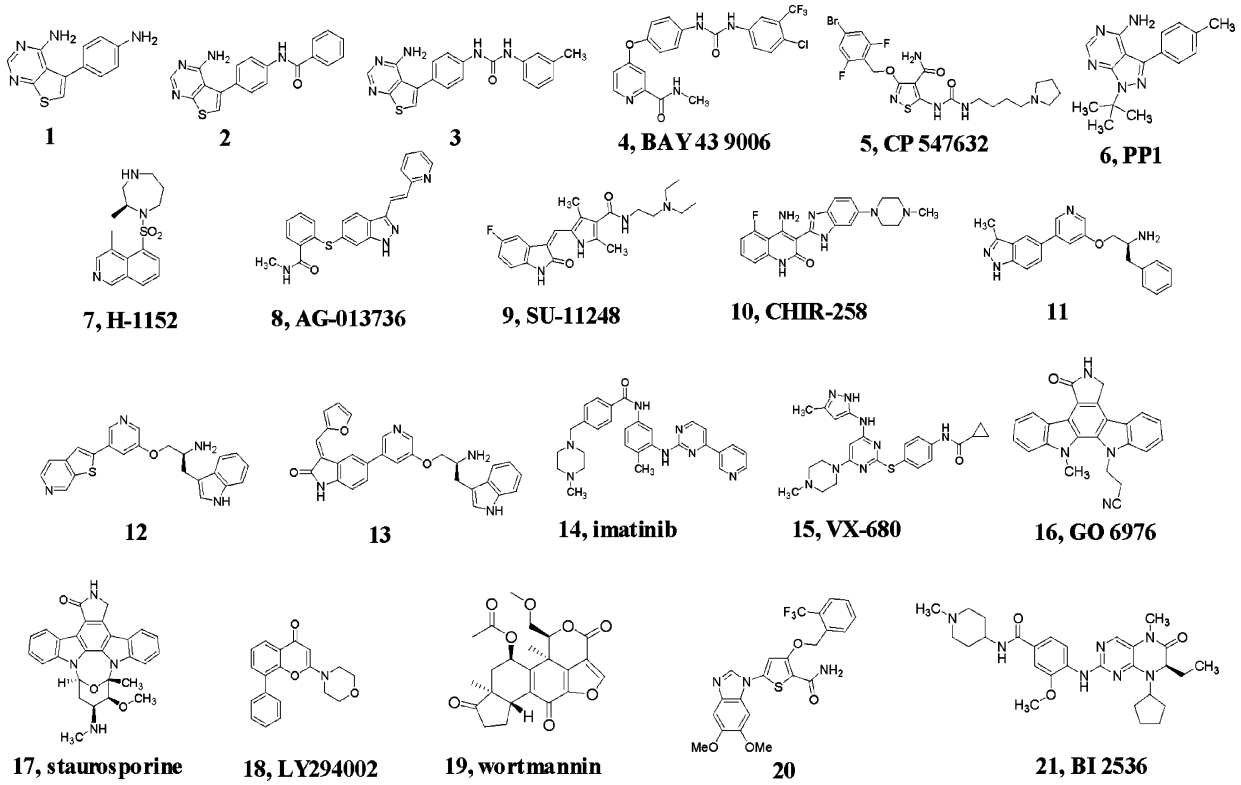

series of three analogous [6.5] thienopyrimidine inhibitors that vary in size and were previously reported to be inhibitors of KDR kinase are represented by compounds **1**, **2**, and **3** (*38*). As the length of the molecule increases (in order of **1** to **2** to **3**), the potency against PLK4 increases, as does the potency against PLK2/3 for the longest compound, compound **3**. Compound **3** is known to target the "inactive" conformation (DFG-out) of KDR (*38*). Therefore, it is possible that some conformational aspects of the inactive and active conformations (DFG-out and DFG-in) of PLK enzymes are one factor in explaining the potencies reported in Table 2. Sorafenib, compound **4**, and Gleevec, compound **14**, target the inactive conformation of their target kinases, bRAF and Abl kinase, respectively. Since these two inhibitors also show some inhibition of PLK4, the possibility of an accessible inactive target conformation, at least for PLK4, is supported.

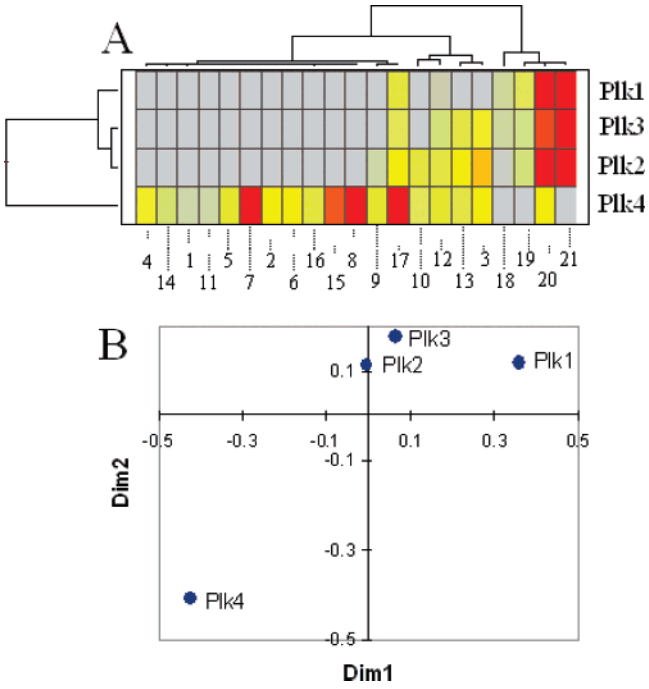

FIGURE 4: Pharmacological similarity of PLK1−4. (A) Hierarchical cluster representation of PLK similarity with respect to ATP-competitive inhibition. All data from Table 2 are represented and colored on a continuous scale: 20 μM (gray), 200 nM (yellow), and 2 nM (red). (B) Multidimensional scaling analysis of the pairwise pharmacological interaction strength for the various PLK isoforms as derived from the inhibitor specificity data in (A). Dim1 and Dim2 are unitless dimensions where distance is inversely proportional to similarity.

The chemical series represented by compounds **11**−**13** has previously been reported to constitute inhibitors of AKT kinase (*45*). Those compounds are known to target the active conformation (DFG-in) of AKT, and by extension they are likely to target the active conformation of PLK. They differ primarily in the nature of the heterocycle used to provide the hydrogen-bonding recognition of the hinge within the ATP-binding site. While no correlate is evident in this limited set of analogues, it is important to note that significant PLK2 and PLK3 activity (submicromolar) can be added to submicromolar PLK4 activity by changing the hinge heterocycle. A related selectivity profile of PLK2/4 over PLK1/3 is also observed for compound **10**.

Compound **19** differs from all other compounds discussed above in exhibiting a pan-PLK inhibitory profile. It has low nanomolar potency against PLK1−3 and also exhibits modest potency against PLK4, indicating that pan-PLK inhibition is achievable with a single small molecule.

Modeling of Amino Acid Differences in the ATP-Binding Site of PLK1−4. As shown in Chart 1 and Table 1, there are significant amino acid differences in the ATP-binding

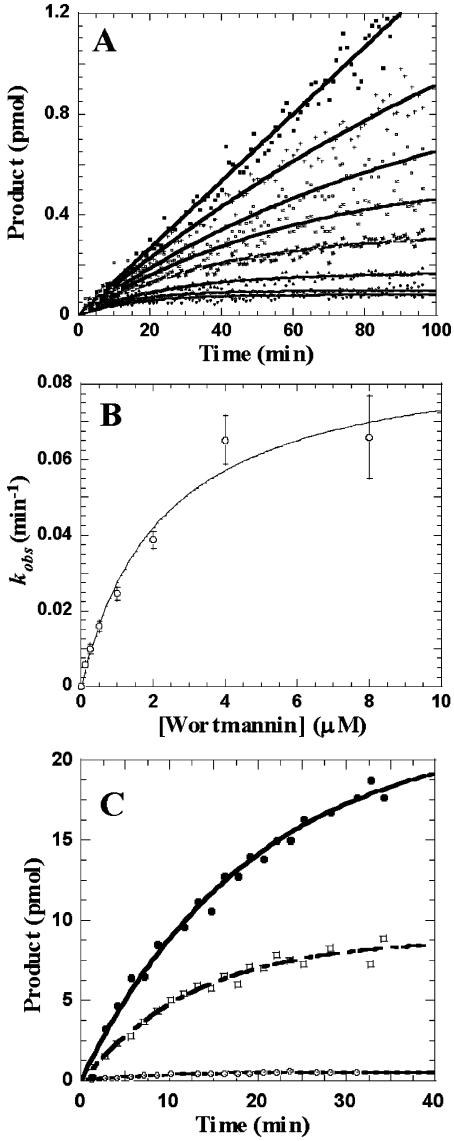

FIGURE 5: Time-dependent inhibition of PLK1 by wortmannin. (A) Progress curves for PLK1-KD activity in the presence of 10 μM ATP and 0 (●), 125 (+), 250 (○), 500 (×), 1000 (■), 2000 (▲), 4000 (◇), or 8000 (▼) nM wortmannin. (B) Secondary plot showing the dependence of the pseudo-first-order rate constant (k_{obs}) at 10 μM ATP on wortmannin concentration. (C) Time-dependent inhibition of fl-PLK1 by 2.5 μM wortmannin in the presence of 5 (○), 125 (□), or 625 (●) μM ATP.

sites of PLK1−4. In particular, PLK4 diverges substantially from PLK1−3. These differences are shown in Figure 7 and are found mainly in the "extended hinge" region (the region of the hinge that is solvent exposed, corresponding to residues 134−140 of PLK1). It is likely that these amino acid differences in the ATP-binding sites of PLK1−4 form at least part of the basis for specificity in the binding interactions.

DISCUSSION

We investigated the pharmacological and functional similarity of the four polo-like kinase family members, comparing specificity in both substrate utilization and ATP site-directed inhibition. We have identified substrate consensus sequences for PLK2, PLK3, and PLK4. We report an expanded consensus sequence for PLK1, which we used to design an optimal PLK1 substrate, PLKtide. We present the pharmacological profile of PLK inhibition by a diverse

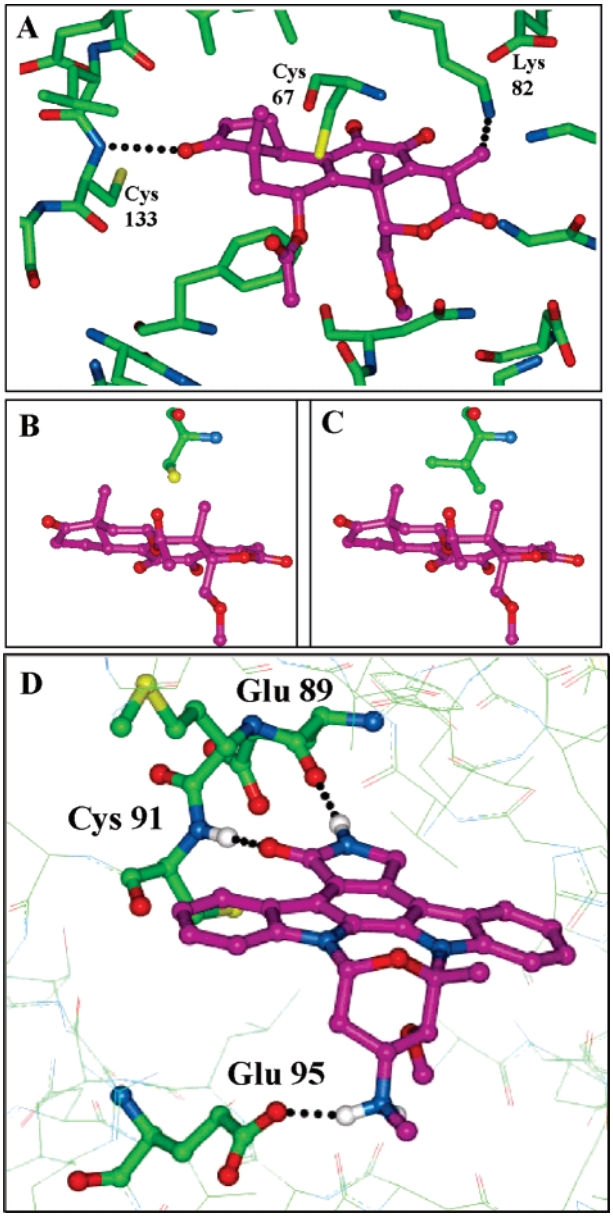

FIGURE 6: Model of wortmannin bound to PLK1. (A) The covalently ring-opened form of wortmannin (purple) is shown bound within the ATP-binding site of PLK1. Shown with black dotted lines are the hydrogen bonds between a carbonyl of wortmannin and the hinge region Cys 133 backbone N−H and the covalent bond between an exocyclic olefin of wortmannin (from ring-opening of the furan) and the Lys 82 side chain amino group (corresponds to Lys 833 of PI3K). (B) Close-up view of wortmannin bound to the PLK active site and the location of one residue, Cys, in PLK1, -2, and -3 (corresponds to Cys 67 in PLK1). (C) Same as panel B but with the equivalent Val in PLK4. The curved lines indicate regions of atomic clash that exist in a docking of wortmannin to PLK4 but do not exist in docking of wortmannin to PLK1−3. (D) Model of staurosporine bound to PLK4. Two hinge hydrogen bonds between the inhibitor and Glu 89 C═O/Cys 91 N−H of PLK4 (corresponds to Glu 131 and Cys 133 of PLK1) are shown with a black dotted line. An additional polar interaction between the positively charged secondary amine of staurosporine and the side chain carboxylate of Glu 95 is shown. Glu 95 of PLK4 corresponds to Ser 137 of PLK1, Ser 166 of PLK2, and Ser 146 of PLK3.

set of kinase inhibitors including several clinical compounds, and we report time-dependent inhibition by two potent and selective PLK inhibitors, wortmannin and BI 2536. Homology models were constructed to provide a three-dimensional context for some of these experimental observations on

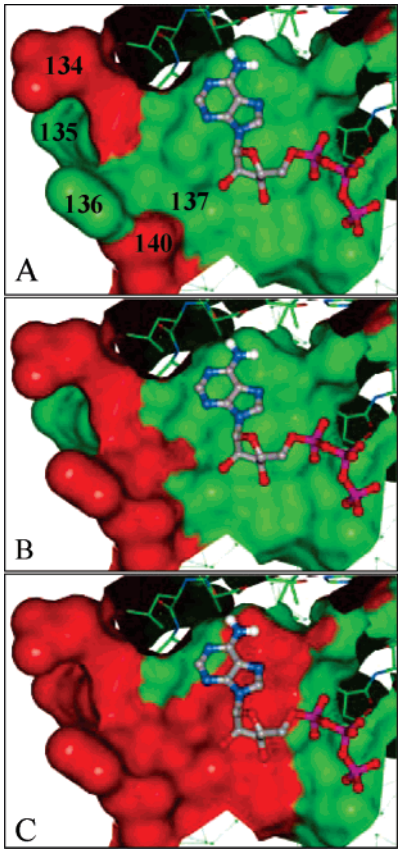

FIGURE 7: Surface of PLK ATP-binding sites highlighting residue variation. (A−C) The surface of the ATP-binding site of PLK1 is shown, with a model of ATP (gray carbons). Amino acids that are different (red) or the same (green) between PLK1 and PLK2 (A), PLK1 and PLK3 (B), or PLK1 and PLK4 (C) are indicated. The most significant region of difference is found in the "extended hinge" region, formed by residues 134−140 of PLK1.

substrates and ligands. While this report was in submission, the crystal structure of a T210V mutant of the PLK-1 catalytic domain appeared in press (*37*). The homology modeling reported in the current study is in excellent agreement with this crystallographic study. PLK1 is a well-validated target, whose pharmacological inhibition holds great promise in the treatment of proliferative diseases including cancer. Insight regarding specificity is essential when targeting the PLK family, particularly with respect to the related kinases PLK2, PLK3, and PLK4. In vivo studies with selective PLK family inhibitors, such as BI 2536, together with knowledge of intrafamily selectivity, should provide clues as to the therapeutic benefit or contraindication associated with inhibiting each member.

PLK Substrate Specificity. Nakajima et al. previously reported a crude substrate consensus sequence, D/E-X-S/T-ψ-X-D/E, for PLK1 as determined by systematic mutagenesis of a Cdc25C-derived peptide (*59*). Our studies provide an expanded PLK1 consensus sequence that is consistent with this report but also indicate additional amino acid preferences extending at least ±7 amino acids from the phosphorylation site. Most notably, there is considerable preference for either an acidic residue or serine at −1 and +3, for serine or hydrophobic at +2, and for acidic residues at −6, +4, +5, +6, and +7 positions. Recently, PLK1 was reported to phosphorylate PBIP1 on Thr 78, to which it subsequently binds via its PBD (*61*). While this substrate has Ala at +1, it lacks acidic residues at the −2 and +3 positions and thus fails to meet the crude consensus requirement (*59*). Yet, this substrate does contain acidic residues at −6, +5, +6, and +7 positions and Ser at −1, all of which are present in the expanded consensus reported here.

Consistent with reported preferences, we observe preferential phosphorylation of Cdc25C Ser 198 and 191 by PLK1 and PLK3, respectively, in a "wild-type" peptide. However, PLK1, PLK2, and PLK3 all showed profound preference for the residue corresponding to Ser 198 in the optimized substrate, PLKtide. Interestingly, mutation or truncation of Ser 198 in PLKtide did not seem to impact residual Ser 191 phosphorylation by PLK1, but did in PLK2 and PLK3. This is consistent with the heightened dependence of PLK1 on a hydrophobic residue at the +1 position. The observation that cJun peptide (Phe at +1) is efficiently phosphorylated by PLK1, but not the other PLKs, further highlights the importance of this position in PLK1 substrates. Modeling of the substrate-binding regions of PLK1−4 (Figure 3E) indicates that there are sites of either similar or divergent pocket residues that are in rough agreement with the substrate variation reported here. The P_1 and P_2 substrate regions were observed to take on significant hydrophobic character in PLK4 relative to PLK1−3, and the corresponding substrate preferences changed from hydrophobic to polar in comparing PLK4 and PLK1−3. The region of protein surrounding the P_{-3} substrate region is variable within the PLK family, with a reversal of substrate residue preference at this position: negatively charged for PLK1−3 and positively charged for PLK4.

In agreement with the homology modeling-based predictions by Lowery et al., PLK4 has a unique and strong preference for Tyr/ψ at the +1 position and for a basic residue at the −3 position (*25*). Modeling predictions further suggested that PLK1, PLK2, and PLK3 would share a similar phosphorylation motif (*25*). Yet, while PLK2 and PLK3 are highly similar in this regard, they differ from PLK1 and do not appear to show a strong preference for a hydrophobic residue in the +1 position, despite the presence of a hydrophobic pocket in their respective models. These data on substrate preference should provide further insight into the cellular targets and functional role of each PLK.

PLK Inhibition by Wortmannin and BI 2536. Although not explicitly stated in the literature, irreversible inhibition of PLK1 by wortmannin is strongly implied since the characterization of wortmannin as an inhibitor of the kinase involved isolation of a wortmannin derivative−PLK1 conjugate by SDS−PAGE (*62*). Moreover, wortmannin is known to be a covalent modifier of its prototypical target, PI3K (*62*, *63*). As an irreversible inhibitor can be expected to impart time-dependent inactivation of its target, a more rigorous analysis is required to characterize wortmannin's inhibition kinetics. Moreover, IC_{50} for such a compound is a function of time and condition; thus it is not meaningful to report an IC_{50} value unless specific details as to assay time and condition are provided. To provide a more meaningful characterization, we investigated the time dependence of PLK inactivation, which indicates that wortmannin is a time-dependent inhibitor of PLK1 but not the other PLK family members. While wortmannin binds to PLK1−3 with similar affinity (1.5−3 μM), it subsequently inactivates PLK1, presumably through covalent modification akin to that

observed for its inactivation of PI3Ks. Further, our data are consistent with wortmannin's having an ATP competitive binding mode. A structural rationalization for this behavior invokes covalent modification of the conserved Lys residue found in all kinases (corresponding to Lys 82 of PLK1) with specificity within the PLK family provided by a nearby Cys/Val residue (corresponding to Cys 67 of PLK1), a residue of difference within the PLK family. Our studies also indicate time-dependent inhibition of PLK1, PLK2, and PLK3 by BI 2536, a compound currently in phase I trials for non-Hodgkin's lymphoma and phase II trials for nonsmall cell lung cancer (*49*, *64*). Long drug-target residence time is reported to enhance target selectivity and prolong in vivo pharmacological action, with many approved drugs involving such mechanism (*65*). Since the current inhibitors of PLK1 also tend to inhibit PLK2 and PLK3, clinical data using advanced PLK inhibitors will provide direct insight into the suitability of PLK2 and PLK3 inhibition in therapy. It will be instructive to compare these efficacy data with those of PLK isoform-specific inhibitors as they become available.

PLK Inhibition by Literature Compounds. Potencies of 21 compounds against the four PLK family members were determined. Almost every possible outcome of isoform selectivity or broad coverage was observed in the library of 21 compounds. This leads to the optimistic viewpoint that clinically useful isoform-targeted inhibitors with drug-like properties can be discovered. The isoform(s) selected for targeting will need to be determined and verified by ongoing biological studies. PLK1 is a current focus of attention, but our current understanding of the biological roles of the individual PLK family members is incomplete. The aspect of protein conformation appears to be one important variable in drug design, as inhibitors that are known to target either active or inactive conformation (DFG-in or DFG-out) of other kinase families both exhibited some inhibition of PLK family members.

PLK Inhibition beyond the ATP-Binding Pocket. The polo-box domain of PLKs also constitutes an attractive target, as inhibitors targeting it should prove relatively selective for this family (*1*, *26*). Moreover, the PBDs serve a functional role in PLK localization, activation, and substrate specificity, providing additional layers of differentiation among the PLK family members (*25*, *27*−*29*, *66*, *67*). While this work is focused on PLK kinase domain relatedness, mechanistic studies of PBD function are ongoing in our laboratory and will be presented in a future report.

PLK Family Relatedness. Historically, PLK1−4 have been grouped together because of (1) the unique presence of an auxiliary PBD (polo-box domain), (2) common motifs from comparison of primary sequences, and (3) overlapping (but not redundant) biological functions. The data from the current study on substrate and inhibitor profiling indicate some divergence within the PLK family. PLK1−3 form a subfamily, distinct from PLK4, with differences in detail observed within the PLK1−3 subfamily. It should be noted, however, that since PLK4 was expressed in *E. coli* and the others in Baculovirus, it is possible that some differences are due to the posttranslational modification of PLK1−3 in the eukaryotic expression system. The purpose of this study was to evaluate what similarities/differences might exist in the PLK family. We feel that we have achieved a qualitative and quantitative initial view of these similarities/differences. It is hoped that further work in drug discovery will be able to exploit those similarities/differences to optimize clinical response. The SAR similarity of PLK1 with PLK2/3 raises important questions for drug discovery. The likelihood a PLK1 inhibitor will also inhibit PLK2/3 increases risk of toxicity. The knowledge of differences between PLK1 and PLK2/3 discussed in this report should aid in the development of PLK1-specific inhibitors if warranted.

ACKNOWLEDGMENT

We thank Dr. Philip Hajduk for providing the MDS analyses of substrate and inhibitor specificity.

REFERENCES

1. Strebhardt, K., and Ullrich, A. (2006) Targeting polo-like kinase 1 for cancer therapy, *Nat. Rev. Cancer 6*, 321−330.
2. Barr, F. A., Sillje, H. H., and Nigg, E. A. (2004) Polo-like kinases and the orchestration of cell division, *Nat. Rev. Mol. Cell Biol. 5*, 429−440.
3. Xie, S., Xie, B., Lee, M. Y., and Dai, W. (2005) Regulation of cell cycle checkpoints by polo-like kinases, *Oncogene 24*, 277−286.
4. van Vugt, M. A., and Medema, R. H. (2005) Getting in and out of mitosis with polo-like kinase-1, *Oncogene 24*, 2844−2859.
5. Liu, X., and Erikson, R. L. (2003) Polo-like kinase (Plk)1 depletion induces apoptosis in cancer cells, *Proc. Natl. Acad. Sci. U.S.A. 100*, 5789−5794.
6. Cogswell, J. P., Brown, C. E., Bisi, J. E., and Neill, S. D. (2000) Dominant-negative polo-like kinase 1 induces mitotic catastrophe independent of Cdc25C function, *Cell Growth Differ. 11*, 615−623.
7. Liu, X., Lei, M., and Erikson, R. L. (2006) Normal cells, but not cancer cells, survive severe Plk1 depletion, *Mol. Cell. Biol. 26*, 2093−2108.
8. Spankuch-Schmitt, B., Wolf, G., Solbach, C., Loibl, S., Knecht, R., Stegmuller, M., von Minckwitz, G., Kaufmann, M., and Strebhardt, K. (2002) Downregulation of human polo-like kinase activity by antisense oligonucleotides induces growth inhibition in cancer cells, *Oncogene 21*, 3162−3171.
9. Gray, P. J., Jr., Bearss, D. J., Han, H., Nagle, R., Tsao, M. S., Dean, N., and Von Hoff, D. D. (2004) Identification of human polo-like kinase 1 as a potential therapeutic target in pancreatic cancer, *Mol. Cancer Ther. 3*, 641−646.
10. Spankuch-Schmitt, B., Bereiter-Hahn, J., Kaufmann, M., and Strebhardt, K. (2002) Effect of RNA silencing of polo-like kinase-1 (PLK1) on apoptosis and spindle formation in human cancer cells, *J. Natl. Cancer Inst. 94*, 1863−1877.
11. Reagan-Shaw, S., and Ahmad, N. (2005) Silencing of polo-like kinase (Plk) 1 via siRNA causes induction of apoptosis and impairment of mitosis machinery in human prostate cancer cells: implications for the treatment of prostate cancer, *FASEB J. 19*, 611−613.
12. Nogawa, M., Yuasa, T., Kimura, S., Tanaka, M., Kuroda, J., Sato, K., Yokota, A., Segawa, H., Toda, Y., Kageyama, S., Yoshiki, T., Okada, Y., and Maekawa, T. (2005) Intravesical administration of small interfering RNA targeting PLK-1 successfully prevents the growth of bladder cancer, *J. Clin. Invest. 115*, 978−985.
13. Spankuch, B., Matthess, Y., Knecht, R., Zimmer, B., Kaufmann, M., and Strebhardt, K. (2004) Cancer inhibition in nude mice after systemic application of U6 promoter-driven short hairpin RNAs against PLK1, *J. Natl. Cancer Inst. 96*, 862−872.
14. Ma, S., Liu, M. A., Yuan, Y. L., and Erikson, R. L. (2003) The serum-inducible protein kinase Snk is a G1 phase polo-like kinase that is inhibited by the calcium- and integrin-binding protein CIB, *Mol. Cancer Res. 1*, 376−384.
15. Yamashita, Y., Kajigaya, S., Yoshida, K., Ueno, S., Ota, J., Ohmine, K., Ueda, M., Miyazato, A., Ohya, K., Kitamura, T., Ozawa, K., and Mano, H. (2001) Sak serine-threonine kinase acts as an effector of Tec tyrosine kinase, *J. Biol. Chem. 276*, 39012−39020.
16. Syed, N., Smith, P., Sullivan, A., Spender, L. C., Dyer, M., Karran, L., O'Nions, J., Allday, M., Hoffmann, I., Crawford, D., Griffin, B., Farrell, P. J., and Crook, T. (2006) Transcriptional silencing

of polo-like kinase 2 (SNK/PLK2) is a frequent event in B-cell malignancies, *Blood 107*, 250−256.
17. Pak, D. T., and Sheng, M. (2003) Targeted protein degradation and synapse remodeling by an inducible protein kinase, *Science 302*, 1368−1373.
18. Kauselmann, G., Weiler, M., Wulff, P., Jessberger, S., Konietzko, U., Scafidi, J., Staubli, U., Bereiter-Hahn, J., Strebhardt, K., and Kuhl, D. (1999) The polo-like protein kinases Fnk and Snk associate with a Ca(2+)- and integrin-binding protein and are regulated dynamically with synaptic plasticity, *EMBO J. 18*, 5528−5539.
19. Burns, T. F., Fei, P., Scata, K. A., Dicker, D. T., and El-Deiry, W. S. (2003) Silencing of the novel p53 target gene Snk/Plk2 leads to mitotic catastrophe in paclitaxel (taxol)-exposed cells, *Mol. Cell. Biol. 23*, 5556−5571.
20. Li, J., Tan, M., Li, L., Pamarthy, D., Lawrence, T. S., and Sun, Y. (2005) SAK, a new polo-like kinase, is transcriptionally repressed by p53 and induces apoptosis upon RNAi silencing, *Neoplasia 7*, 312−323.
21. Bahassi el, M., Hennigan, R. F., Myer, D. L., and Stambrook, P. J. (2004) Cdc25C phosphorylation on serine 191 by Plk3 promotes its nuclear translocation, *Oncogene 23*, 2658−2663.
22. Myer, D. L., Bahassi el, M., and Stambrook, P. J. (2005) The Plk3-Cdc25 circuit, *Oncogene 24*, 299−305.
23. Xie, S., Wang, Q., Wu, H., Cogswell, J., Lu, L., Jhanwar-Uniyal, M., and Dai, W. (2001) Reactive oxygen species-induced phosphorylation of p53 on serine 20 is mediated in part by polo-like kinase-3, *J. Biol. Chem. 276*, 36194−36199.
24. Habedanck, R., Stierhof, Y. D., Wilkinson, C. J., and Nigg, E. A. (2005) The polo kinase Plk4 functions in centriole duplication, *Nat. Cell Biol. 7*, 1140−1146.
25. Lowery, D. M., Lim, D., and Yaffe, M. B. (2005) Structure and function of polo-like kinases, *Oncogene 24*, 248−259.
26. McInnes, C., Mezna, M., and Fischer, P. M. (2005) Progress in the discovery of polo-like kinase inhibitors, *Curr. Top. Med. Chem. 5*, 181−197.
27. Elia, A. E., Rellos, P., Haire, L. F., Chao, J. W., Ivins, F. J., Hoepker, K., Mohammad, D., Cantley, L. C., Smerdon, S. J., and Yaffe, M. B. (2003) The molecular basis for phosphodependent substrate targeting and regulation of Plks by the polo-box domain, *Cell 115*, 83−95.
28. Elia, A. E., Cantley, L. C., and Yaffe, M. B. (2003) Proteomic screen finds pSer/pThr-binding domain localizing Plk1 to mitotic substrates, *Science 299*, 1228−1231.
29. Yaffe, M. B., and Smerdon, S. J. (2004) The use of in vitro peptide-library screens in the analysis of phosphoserine/threonine-binding domain structure and function, *Annu. Rev. Biophys. Biomol. Struct. 33*, 225−244.
30. Manning, G., Whyte, D. B., Martinez, R., Hunter, T., and Sudarsanam, S. (2002) The protein kinase complement of the human genome, *Science 298*, 1912−1934.
31. Hanks, S. K., Quinn, A. M., and Hunter, T. (1988) The protein kinase family: conserved features and deduced phylogeny of the catalytic domains, *Science 241*, 42−52.
32. Simmons, D. L., Neel, B. G., Stevens, R., Evett, G., and Erikson, R. L. (1992) Identification of an early-growth-response gene encoding a novel putative protein kinase, *Mol. Cell. Biol. 12*, 4164−4169.
33. Donohue, P. J., Alberts, G. F., Guo, Y., and Winkles, J. A. (1995) Identification by targeted differential display of an immediate early gene encoding a putative serine/threonine kinase, *J. Biol. Chem. 270*, 10351−10357.
34. Vieth, M., Higgs, R. E., Robertson, D. H., Shapiro, M., Gragg, E. A., and Hemmerle, H. (2004) Kinomics-structural biology and chemogenomics of kinase inhibitors and targets, *Biochim. Biophys. Acta 1697*, 243−257.
35. Frye, S. V. (1999) Structure-activity relationship homology (SARAH): a conceptual framework for drug discovery in the genomic era, *Chem. Biol. 6*, R3−R7.
36. Davies, S. P., Reddy, H., Caivano, M., and Cohen, P. (2000) Specificity and mechanism of action of some commonly used protein kinase inhibitors, *Biochem. J. 351*, 95−105.
37. Kothe, M., Kohls, D., Low, S., Coli, R., Cheng, A. C., Jacques, S. L., Johnson, T. L., Lewis, C., Loh, C., Nonomiya, J., Sheils, A. L., Verdries, K. A., Wynn, T. A., Kuhn, C., and Ding, Y. H. (2007) Structure of the catalytic domain of human polo-like kinase 1(,), *Biochemistry* (in press).
38. Dai, Y., Guo, Y., Frey, R. R., Ji, Z., Curtin, M. L., Ahmed, A. A., Albert, D. H., Arnold, L., Arries, S. S., Barlozzari, T., Bauch, J. L., Bouska, J. J., Bousquet, P. F., Cunha, G. A., Glaser, K. B., Guo, J., Li, J., Marcotte, P. A., Marsh, K. C., Moskey, M. D., Pease, L. J., Stewart, K. D., Stoll, V. S., Tapang, P., Wishart, N., Davidsen, S. K., and Michaelides, M. R. (2005) Thienopyrimidine ureas as novel and potent multitargeted receptor tyrosine kinase inhibitors, *J. Med. Chem. 48*, 6066−6083.
39. Larson, E. R., Noe, M. C., and Gant, T. G. (1999) WO1999062890.
40. Beebe, J. S., Jani, J. P., Knauth, E., Goodwin, P., Higdon, C., Rossi, A. M., Emerson, E., Finkelstein, M., Floyd, E., Harriman, S., Atherton, J., Hillerman, S., Soderstrom, C., Kou, K., Gant, T., Noe, M. C., Foster, B., Rastinejad, F., Marx, M. A., Schaeffer, T., Whalen, P. M., and Roberts, W. G. (2003) Pharmacological characterization of CP-547,632, a novel vascular endothelial growth factor receptor-2 tyrosine kinase inhibitor for cancer therapy, *Cancer Res. 63*, 7301−7309.
41. Ewanicki, B., Flahive, E., Kasparian, A., Mitchell, M., Perry, M., O'Neill-Slawecki, S., Sach, N., Saenz, J., Shi, B., Stankovic, N., Srirangam, J., Tian, Q., and Yu, S. (2006) US2005264440.
42. Inai, T., Mancuso, M., Hashizume, H., Baffert, F., Haskell, A., Baluk, P., Hu-Lowe, D. D., Shalinsky, D. R., Thurston, G., Yancopoulos, G. D., and McDonald, D. M. (2004) Inhibition of vascular endothelial growth factor (VEGF) signaling in cancer causes loss of endothelial fenestrations, regression of tumor vessels, and appearance of basement membrane ghosts, *Am. J. Pathol. 165*, 35−52.
43. Renhowe, P. A., Pecchi, S., Machajewski, T. D., Shafer, C. M., Taylor, C., McCrea, W. R., McBride, C., Jazan, E., and Heise, C. (2003) WO2003087095.
44. Trudel, S., Li, Z. H., Wei, E., Wiesmann, M., Chang, H., Chen, C., Reece, D., Heise, C., and Stewart, A. K. (2005) CHIR-258, a novel, multitargeted tyrosine kinase inhibitor for the potential treatment of t(4;14) multiple myeloma, *Blood 105*, 2941−2948.
45. Woods, K. W., Fischer, J. P., Claiborne, A., Li, T., Thomas, S. A., Zhu, G. D., Diebold, R. B., Liu, X., Shi, Y., Klinghofer, V., Han, E. K., Guan, R., Magnone, S. R., Johnson, E. F., Bouska, J. J., Olson, A. M., de Jong, R., Oltersdorf, T., Luo, Y., Rosenberg, S. H., Giranda, V. L., and Li, Q. (2006) Synthesis and SAR of indazole-pyridine based protein kinase B/Akt inhibitors, *Bioorg. Med. Chem. 14*, 6832−6846.
46. Andrews, C. W., III, Cheung, M., Davis-Ward, R. G., Drewry, D. H., Emmitte, K. A., Hubbard, R. D., Kuntz, K. W., Linn, J. A., Mook, R. A., Smith, G. K., and Veal, J. M. (2004) WO2004014899.
47. Lansing, T. J., McConnell, R. T., Duckett, D. R., Spehar, G. M., Knick, V. B., Hassler, D. F., Noro, N., Furuta, M., Emmitte, K. A., Gilmer, T. M., Mook, R. A., Jr., and Cheung, M. (2007) In vitro biological activity of a novel small-molecule inhibitor of polo-like kinase 1, *Mol. Cancer Ther. 6*, 450−459.
48. Hoffmann, M., Grauert, M., Brandl, T., Breitfelder, S., Eickmeier, C., Steegmaier, M., Schnapp, G., Baum, A., Quant, J. J., Solca, F., and Colbatzky, F. (2004) WO2004076454.
49. Steegmaier, M., Hoffmann, M., Baum, A., Lenart, P., Petronczki, M., Krssak, M., Gurtler, U., Garin-Chesa, P., Lieb, S., Quant, J., Grauert, M., Adolf, G. R., Kraut, N., Peters, J. M., and Rettig, W. J. (2007) BI 2536, a potent and selective inhibitor of polo-like kinase 1, inhibits tumor growth in vivo, *Curr. Biol. 17*, 316−322.
50. Cheng, Y., and Prusoff, W. H. (1973) Relationship between the inhibition constant (K1) and the concentration of inhibitor which causes 50 per cent inhibition (I50) of an enzymatic reaction, *Biochem. Pharmacol. 22*, 3099−3108.
51. Gray, P. J., and Duggleby, R. G. (1989) Analysis of kinetic data for irreversible enzyme inhibition, *Biochem. J. 257*, 419−424.
52. Kati, W. M., Sham, H. L., McCall, J. O., Montgomery, D. A., Wang, G. T., Rosenbrook, W., Miesbauer, L., Buko, A., and Norbeck, D. W. (1999) Inhibition of 3C protease from human rhinovirus strain 1B by peptidyl bromomethylketone hydrazides, *Arch. Biochem. Biophys. 362*, 363−375.
53. Copeland, R. A. (2005) *Evaluation of Enzyme Inhibitors in Drug Discovery: A Guide for Medicinal Chemists and Pharmacologists*, Wiley, New York.
54. Paolini, G. V., Shapland, R. H., van Hoorn, W. P., Mason, J. S., and Hopkins, A. L. (2006) Global mapping of pharmacological space, *Nat. Biotechnol. 24*, 805−815.
55. Lin, C. Y., Madsen, M. L., Yarm, F. R., Jang, Y. J., Liu, X., and Erikson, R. L. (2000) Peripheral Golgi protein GRASP65 is a target of mitotic polo-like kinase (Plk) and Cdc2, *Proc. Natl. Acad. Sci. U.S.A. 97*, 12589−12594.

56. Toyoshima-Morimoto, F., Taniguchi, E., and Nishida, E. (2002) Plk1 promotes nuclear translocation of human Cdc25C during prophase, *EMBO Rep. 3*, 341−348.
57. Toyoshima-Morimoto, F., Taniguchi, E., Shinya, N., Iwamatsu, A., and Nishida, E. (2001) Polo-like kinase 1 phosphorylates cyclin B1 and targets it to the nucleus during prophase, *Nature 410*, 215−220.
58. Yarm, F. R. (2002) Plk phosphorylation regulates the microtubule-stabilizing protein TCTP, *Mol. Cell. Biol. 22*, 6209−6221.
59. Nakajima, H., Toyoshima-Morimoto, F., Taniguchi, E., and Nishida, E. (2003) Identification of a consensus motif for Plk (polo-like kinase) phosphorylation reveals Myt1 as a Plk1 substrate, *J. Biol. Chem. 278*, 25277−25280.
60. Walker, E. H., Pacold, M. E., Perisic, O., Stephens, L., Hawkins, P. T., Wymann, M. P., and Williams, R. L. (2000) Structural determinants of phosphoinositide 3-kinase inhibition by wortmannin, LY294002, quercetin, myricetin, and staurosporine, *Mol. Cell 6*, 909−919.
61. Kang, Y. H., Park, J. E., Yu, L. R., Soung, N. K., Yun, S. M., Bang, J. K., Seong, Y. S., Yu, H., Garfield, S., Veenstra, T. D., and Lee, K. S. (2006) Self-regulated Plk1 recruitment to kinetochores by the Plk1-PBIP1 interaction is critical for proper chromosome segregation, *Mol. Cell 24*, 409−422.
62. Wipf, P., and Halter, R. J. (2005) Chemistry and biology of wortmannin, *Org. Biomol. Chem. 3*, 2053−2061.
63. Vlahos, C. J., Matter, W. F., Hui, K. Y., and Brown, R. F. (1994) A specific inhibitor of phosphatidylinositol 3-kinase, 2-(4-morpholinyl)-8-phenyl-4H-1-benzopyran-4-one (LY294002), *J. Biol. Chem. 269*, 5241−5248.
64. Steegmaier, M., Baum, A., Solca, F., Peters, J., Grauert, M., and Hoffmann, M. (2005) A potent and highly selective inhibiotr of polo-like kinase 1 (Plk1), induces mitotic arrest and apoptosis in a broad spectrum of tumor cell lines, *Clin. Cancer Res. 11* (Suppl.), 9147.
65. Copeland, R. A., Pompliano, D. L., and Meek, T. D. (2006) Drug-target residence time and its implications for lead optimization, *Nat. Rev. Drug Discov. 5*, 730−739.
66. Jang, Y. J., Lin, C. Y., Ma, S., and Erikson, R. L. (2002) Functional studies on the role of the C-terminal domain of mammalian polo-like kinase, *Proc. Natl. Acad. Sci. U.S.A. 99*, 1984−1989.
67. Cheng, K. Y., Lowe, E. D., Sinclair, J., Nigg, E. A., and Johnson, L. N. (2003) The crystal structure of the human polo-like kinase-1 polo box domain and its phospho-peptide complex, *EMBO J. 22*, 5757−5768.

BI7008745